International Journal of Innovative Research in Advanced Engineering (IJIRAE)
Volume 1 Issue 2 (April 2014)

Comparison of Explicit Finite Difference Model and Galerkin Finite Element Model for Simulation of Groundwater Flow

N.H.Kulkarni *
Associate Professor,
Dept. of Civil& Water Management Engg.,SGGSIE&T,Nanded-431606.

A.K.Rastogi
Professor
Dept. of Civil Engg. IIT Bombay- 400076.

Abstract— This paper describes Galerkin finite element (FEFLOW) models for the simulation of groundwater flow in two-dimensional, transient, unconfined groundwater flow systems. This study involves validation of FEFLOW model with reported analytical solutions and also comparison of reported Explicit Finite Difference Model for groundwater flow simulation (FDFLOW). The model is further used to obtain the space and time distribution of groundwater head for the reported synthetic test case. The effect of time step size, space discretizations, pumping rates is analyzed on model results.

Keywords—Flow simulation model, Unconfined groundwater flow, Space - time distribution of groundwater head, Validation of numerical groundwater flow model

I. INTRODUCTION

Numerical models of groundwater flow are properly conceptualized version of a complex aquifer system which approximates the flow phenomenon.. The approximations in the numerical models are effected in through the set of assumptions pertaining to the geometry of the domain, ways the heterogeneities are smoothed out, the nature of the porous medium, properties of the fluid and the type of the flow regime. The complex aquifer system is treated as a continuum, which implies that the fluid and solid matrix variables are continuously defined at every point in the aquifer domain. The continuum is viewed as a network of several representative elementary volumes, each representing a portion of the entire volume of an aquifer with average fluid and solid properties taken over it and assigned to the nodes of superimposed grid used for the discretization of the domain. The numerical models greatly help in analyzing the implications of proposed excitations on the response of the aquifer systems. They are advantageous than the conventional physical and analog models in respect of expressing the interactions of simultaneous physical processes and their influences on each other by set of constitutive relationships. These models also help in synthesizing field information and handling the large amount of input data in regional scale problems [*Wang and Anderson, 1982*]**.** Numerical models are applied either in an interpretive sense to gain insight into controlling the aquifer parameters in a site-specific setting or in generic sense to formulate regional regulatory guidelines and act as screening tools to identify regions suitable for some proposed action such as. artificial recharge. The constitution of a groundwater flow model consists of the governing equation of groundwater flow which is obtained by combining the flow continuity equation based on conservation of mass with the Darcy's law based on conservation of momentum. The flow equation is described with the unsteady or steady state of the flow regime.

Pinder and Bredehoeft (1968) used alternating direction implicit finite difference scheme to solve the groundwater flow equation. This numerical scheme is implemented for two-dimensional groundwater flow in heterogeneous and anisotropic confined aquifer. The results of the implementation of this model are in close agreement with the Theis analytical solutions.

Narasimhan and Witherspopoon (1976) developed an integrated finite difference model for analyzing the transient groundwater flow in variably saturated heterogeneous aquifer. A computer program TRUST is developed to analyze transient groundwater motion for variably saturated deformable heterogeneous and multidimensional aquifer system. The program has been validated against analytical solutions, experimental data and field results. Pinder and Frind (1972) developed the Galerkin finite element model to simulate two-dimensional groundwater flow in a leaky aquifer. The accuracy of model results is compared with the finite difference results and it is found that both the results are in close agreement with each other. Thomson et al. (1984) presented a Galerkin finite element model using Picard and Newton-Raphson algorithms designed for solution of non-linear groundwater flow equation. The model uses both triangular and rectangular finite elements for aquifer discretization. The influence area coefficient technique is used instead of conventional numerical integration scheme to obtain element matrices. It is found that this new technique is successful in reduction of computational cost. Serigo et al. (2004) developed the discontinuous Galerkin method which uses a finite-element discretization of the groundwater flow domain. Their model used an interpolation function of an arbitrary order is for each element of the domain. The independent choice of an interpolation functions in each element permits discontinuities in transmissivity in the flow domain. This formulation is shown to be of high order accuracy and particularly suitable for accurately calculating the flow field in porous media. Simulations are presented in terms of streamlines in a two-dimensional aquifer and compared with the solutions obtained from standard finite-element method and a mixed finite-element method. Numerical simulations show that the discontinuous Galerkin approximation is more efficient than the standard finite-element method in computing fluxes and streamlines for a given accuracy.

Kulkarni N.H. et al. (2012) discussed the validation of numerical groundwater flow simulation models and analyzed the effect of variation of aquifer and flow parameters on numerical model solutions.

II. GROUNDWATER FLOW EQUATION

The governing equation of two-dimensional, horizontal, and transient groundwater flow in homogeneous, isotropic and unconfined aquifer is given as [Illangasekare and Doll, 1989]

$$S_y \frac{\partial h}{\partial t} = T_{xx} \frac{\partial^2 h}{\partial x^2} + T_{yy} \frac{\partial^2 h}{\partial y^2} + \sum_{i=1}^{n_w} Q_i \delta(x_o - x_i, y_o - y_i) + \sum_{j=1}^{n_p} q_j \qquad (1)$$

where S_y is the specific yield, [dimensionless]; h is the hydraulic head averaged over vertical, [L]; t is the time, [T]; T_{xx} and T_{yy} are components of the transmissiviy tensor, [L^2/T] which are approximated as $T_{xx} \approx K_{xx} h$ and $T_{yy} \approx K_{yy} h$, provided the change in the head in unconfined aquifer is negligible as compared to its saturated thickness [Illangsekare and Doll, 1989]; K_{xx} and K_{yy} are components of the hydraulic conductivity tensor, [L/T]; x and y are spatial coordinates, [L]; Q_i is the pumping rate when ($Q_i < 0$) and injection rate when ($Q_i > 0$) at i th pumping and / or injection well, [L^3/T]; n_w is the number of pumping and/or injection wells in the domain; n_p is the number of nodes in the domain with distributed discharge and/or recharge; $\delta(x_o - x_i, y_o - y_i)$ is the Dirac delta function; x_o and y_o are the Cartesian coordinates of the origin , [L]; x_i and y_i are the coordinates of i th pumping and / or injection well, [L]; q_j is the distributed discharge rate when ($q_j < 0$)and recharge rate when ($q_j > 0$) at j th nodes with distributed discharge and/or recharge, [L/T]. Equation (1) is subject to the following initial condition which is given as

$$h(x, y, 0) = h_0 \qquad (x, y) \in \Omega \qquad (2)$$

Where h_0 is the initial head over the entire flow domain, [L] and Ω is the flow domain, [L^2]. Equation (1) is subject to the Dirichlet type of boundary condition which is given as

$$h(x, y, t) = h_1 \qquad (x, y) \in \Gamma_1 ; \; t \geq 0 \qquad (3)$$

Where h_1 is the prescribed head over aquifer domain boundary Γ_1 , [L].The Neumann boundary condition with zero groundwater flux can be given as

$$\left[\{q_b(x, y, t)\} - [T]\nabla h(x, y, t)\right] \cdot \{n\} = 0 \qquad (x, y) \in \Gamma_2 ; \; t \geq 0 \qquad (4)$$

Where q_b is the specified groundwater flux across boundary Γ_2 ,[L/T]; $[T]\nabla h$ is the groundwater flux across the boundary Γ_2 , [L/T] and n is normal unit vector in outward direction.

III. FDFLOW MODEL

The explicit finite difference method is employed in FDFLOW model to solve the Equation (1). In this model the unknown nodal head at next time level is explicitly computed from the four neighboring nodes with known heads at the previous time level. The explicit finite difference scheme is adopted because it is computationally efficient than the alternating direction implicit finite difference scheme but it has the restriction of the size of time step used in simulation. However, the stability of the solutions can be ensured by constraining the length of a time step. In this model the entire aquifer domain is discretized into rectangular computational cells by superimposing the mesh centered finite difference grid over the domain. The computational cells are formed around the intersection points of grid column and row lines which are referred to as a nodes. Thus each node with grid column index i and grid row index j represents a computational cell. The size of each rectangular computational cell is Δx and Δy in x- and y- directions respectively. In FDFLOW model, the spatial derivatives and temporal derivative in Equation (1) are approximated by central finite difference and forward difference schemes respectively which will result into the following equation

$$\frac{S_{y_{i,j}}(h_{i,j}^{t+\Delta t} - h_{i,j}^{t})}{\Delta t} = \frac{(T_{xx_{i,j}}(h_{i+1,j}^{t} - 2h_{i,j}^{t} + h_{i-1,j}^{t}))}{\Delta x^2} + \frac{(T_{yy_{i,j}}(h_{i,j+1}^{t} - 2h_{i,j}^{t} + h_{i-1,j}^{t}))}{\Delta y^2} + \frac{Q_{i,j}}{\Delta x \Delta y} + q_{i,j} \qquad (5)$$

Where Δt the time step size, [T]; t and $t + \Delta t$ are the previous and next time levels, [T] and i, j is the nodal index. The various terms of the Equation (3.11) are rearranged in such a way that all the known nodal heads should appear on one side of the equation and thus the expression for the nodal head at the next time level can be given as

$$h_{i,j}^{t+\Delta t} = h_{i,j}^{t} + \frac{T_{xx_{i,j}}\Delta t}{S_{y_{i,j}}\Delta x^2}\left(h_{i+1,j}^{t} - 2h_{i,j}^{t} + h_{i-1,j}^{t}\right) + \frac{T_{yy_{i,j}}\Delta t}{S_{y_{i,j}}\Delta y^2}\left(h_{i,j+1}^{t} - 2h_{i,j}^{t} + h_{i-1,j}^{t}\right) + \frac{\Delta t Q_{i,j}}{S_{y_{i,j}}\Delta x\Delta y} + \frac{\Delta t q_{i,j}}{S_{y_{i,j}}} \qquad (6)$$

The Equation (5) when written for all the nodes 1,2 .. N of the aquifer domain it will constitute the system of linear algebraic equations which is expressed in the matrix form as

$$\begin{Bmatrix} h_1^{t+\Delta t} \\ h_2^{t+\Delta t} \\ \cdot \\ \cdot \\ h_N^{t+\Delta t} \end{Bmatrix} = \begin{bmatrix} \left(\frac{T_{xx_1}\Delta t}{S_{y_1}\Delta x^2}\right) & 0 & 0 & 0 \\ 0 & \left(\frac{T_{xx_2}\Delta t}{S_{y_2}\Delta x^2}\right) & 0 & 0 \\ 0 & 0 & - & 0 \\ 0 & 0 & 0 & \left(\frac{T_{xx_N}\Delta t}{S_{y_N}\Delta x^2}\right) \end{bmatrix} + \begin{bmatrix} \left(\frac{T_{yy_1}\Delta t}{S_{y_1}\Delta y^2}\right) & 0 & 0 & 0 \\ 0 & \left(\frac{T_{yy_2}\Delta t}{S_{y_2}\Delta y^2}\right) & 0 & 0 \\ 0 & 0 & - & 0 \\ 0 & 0 & 0 & \left(\frac{T_{yy_N}\Delta t}{S_{y_N}\Delta y^2}\right) \end{bmatrix} \begin{Bmatrix} h_1^{t} \\ h_2^{t} \\ \cdot \\ \cdot \\ h_N^{t} \end{Bmatrix} \qquad (7)$$

Thus the unknown nodal head vector in Equation (7) is solved using the direct matrix inversion technique available in MAT-LAB environment.

IV. **FEFLOW MODEL**

This model employs the Galerkin finite element technique for computing the head distribution in aquifer. In this method the trial solution of the head is substituted into the Equation (1) which results into the residual. By using the weighting functions as the shape functions the weighted residual is integrated and forced to zero to yield the system of linear equations. The set of the linear equations is solved to get the nodal head distribution. The groundwater flow domain is discretized into finite number of nodes using a triangular finite element mesh. Each node of the domain is identified by an index L and the finite element by an index e. The three nodes of a finite element are labeled as i, j and k in either clockwise or anticlockwise manner. The time domain is discretized into finite number of discrete time steps. The size of each time step is Δt. The trial solution of the groundwater head to be used in finite element formulation is given as

$$\hat{h}(x, y, t) = \sum_{L=1}^{N} h_L(t)\, N_L(x, y) \qquad (8)$$

Where $\hat{h}$ is the trial solution of groundwater head, [L]; N is the total number of nodes in the flow domain; h_L is the nodal groundwater head at any time t, [L]; N_L is the linear shape function at any point (x, y) in the aquifer domain. The shape function is defined piecewise but in continuous manner over entire flow domain which ranges from 0 to 1.The trial solution is substituted for unknown nodal head h in the Equation (1) which results into the residual of groundwater head which is expressed as

$$\varepsilon^h(x,y,t) = T_{xx}\frac{\partial^2 \hat{h}}{\partial x^2} + T_{yy}\frac{\partial^2 \hat{h}}{\partial y^2} + \sum_{i=1}^{n_w} Q_i\delta(x_o - x_i, y_o - y_i) + \sum_{j=1}^{n_p} q_j - S_y\frac{\partial \hat{h}}{\partial t} \qquad (9)$$

Where ε^h is the residual of groundwater head at any point (x, y) and at time t; [L].The residual of the head is weighted and integrated over entire flow domain to obtain the nodal head distribution. The integral of the weighted head residual is forced to zero to yield the system of algebraic equations and the same is given as

$$\iint_{\Omega}\left(T_{xx}\frac{\partial^2 \hat{h}}{\partial x^2} + T_{yy}\frac{\partial^2 \hat{h}}{\partial y^2} + \sum_{i=1}^{n_w} Q_i\delta(x_o - x_i, y_o - y_i) + \sum_{j=1}^{n_p} q_j - S_y\frac{\partial \hat{h}}{\partial t}\right) W_L\, dx\, dy = 0 \qquad (10)$$

Where W_L is the weighting function at a node L. The integral of Equation (7) is evaluated using Green's function which reduces the second order derivatives terms to the first order derivatives and is expressed as

(11)

$$\iint_{\Omega}\left(T_{xx}\frac{\partial \hat{h}}{\partial x}\frac{\partial W_L}{\partial x} + T_{yy}\frac{\partial \hat{h}}{\partial y}\frac{\partial W_L}{\partial y}\right) dx\, dy - \iint_{\Omega}\left(S_y\frac{\partial \hat{h}}{\partial t}\right) W_L\, dx\, dy +$$

$$\iint_{\Omega}\left(\sum_{i=1}^{n_w} Q_i\delta(x_o - x_i, y_o - y_i) + \sum_{j=1}^{n_p} q_j\right) W_L\, dx\, dy + \int_{\Gamma}\left(T_{xx}\frac{\partial \hat{h}}{\partial x}n_x + T_{yy}\frac{\partial \hat{h}}{\partial y}n_y\right) W_L\, d\sigma = 0$$

Where $d\sigma$ is generalized variable representing distance along the boundary, [L].The Equation (8) can be expressed in the following form by substituting N_L for W_L and given as

$$\iint_{\Omega}\left(T_{xx}\frac{\partial \hat{h}}{\partial x}\frac{\partial N_L}{\partial x}+T_{yy}\frac{\partial \hat{h}}{\partial y}\frac{\partial N_L}{\partial y}\right)dxdy-\iint_{\Omega}\left(S_y\frac{\partial \hat{h}}{\partial t}\right)N_L\,dxdy+$$

$$\iint_{\Omega}\left(\sum_{i=1}^{n_w}Q_i\delta(x_o-x_i,y_o-y_i)+\sum_{j=1}^{n_p}q_j\right)N_L\,dxdy+\int_{\Gamma}\left(T_{xx}\frac{\partial \hat{h}}{\partial x}n_x+T_{yy}\frac{\partial \hat{h}}{\partial y}n_y\right)N_L\,d\sigma=0 \quad (12)$$

The Equation (9) can be written expressed for individual element as

$$\sum_{e=1}^{M}\iint_{e}\left(\frac{\partial \hat{h}_L^e}{\partial x}\frac{\partial N_L^e}{\partial x}+\frac{\partial \hat{h}_L^e}{\partial y}\frac{\partial N_L^e}{\partial y}\right)dxdy+\sum_{e=1}^{M}\iint_{e}\left(\frac{S_y{}^e}{T^e}\frac{\partial \hat{h}_L^e}{\partial t}\right)N_L^e\,dxdy=$$

$$\sum_{e=1}^{M}\iint_{e}\left(\sum_{i=1}^{n_w}Q_i^e\delta(x_o-x_i,y_o-y_i)+\sum_{j=1}^{n_p}q_j^e\right)N_L^e\,dxdy+\sum_{e=1}^{M}\int_{\Gamma}\frac{1}{T^e}\left(\frac{\partial \hat{h}_L^e}{\partial x}n_x+\frac{\partial \hat{h}_L^e}{\partial y}n_y\right)N_L^e\,d\sigma^e \quad (13)$$

Applying the numerical integration for the various terms of Equation (10) the following system of linear equations is obtained and the same can be written as

$$\left([\boldsymbol{G}]+\frac{1}{\Delta t}[\boldsymbol{P}]\right)\left\{h_{i,j}^{t+\Delta t}\right\}=\left(\frac{1}{\Delta t}[\boldsymbol{P}]\right)\left\{h_{i,j}^{t}\right\}+\{\boldsymbol{B}\}+\{\boldsymbol{f}\} \quad (14)$$

Where $[\boldsymbol{G}]$ is the global conductance matrix which is formed by assembling the elemental conductance matrices $\left[G_L^e\right]$ that can be expressed as

$$\left[G_L^e\right]=\iint_{e}\left(\frac{\partial \hat{h}_L^e}{\partial x}\frac{\partial N_L^e}{\partial x}+\frac{\partial \hat{h}_L^e}{\partial y}\frac{\partial N_L^e}{\partial y}\right)dxdy=\frac{1}{4A^e}\begin{bmatrix} b_1^eb_1^e & b_1^eb_j^e & b_1^eb_k^e \\ b_j^eb_1^e & b_j^eb_j^e & b_j^eb_k^e \\ b_k^eb_1^e & b_k^eb_j^e & b_k^eb_k^e \end{bmatrix}+\begin{bmatrix} c_1^ec_1^e & c_1^ec_j^e & c_1^ec_k^e \\ c_j^ec_1^e & c_j^ec_j^e & c_j^ec_k^e \\ c_k^ec_1^e & c_k^ec_j^e & c_k^ec_k^e \end{bmatrix} \quad (15)$$

$[\boldsymbol{P}]$ is the global storage matrix which is assembled from elemental storage matrices $\left[P_L^e\right]$ that can be given as

$$\left[P_L^e\right]=\iint_{e}\frac{\partial \hat{h}_L^e}{\partial t}N_L^e\frac{S_y^e}{T^e}\,dxdy=\iint_{e}N_L^eN_L^e\frac{S_y^e}{T^e}\,dxdy=\frac{S_y^e}{T^e}\frac{A^e}{12}\begin{bmatrix}2&1&1\\1&2&1\\1&1&2\end{bmatrix} \quad \because L=i\neq j\neq k \quad (16)$$

$\{\boldsymbol{B}\}$ is the global load vector which is assembled from elemental load vectors $\left\{B_L^e\right\}$ that can be given as

$$\left\{B_L^e\right\}=\iint_{e}\left(\sum_{i=1}^{n_w}Q_i^e\delta(x_o-x_i,y_o-y_i)+\sum_{j=1}^{n_p}q_j^e\right)N_L^e\,dxdy=\left(\frac{Q^e}{3T^e}+\frac{q^eA^e}{3T^e}\right)\begin{bmatrix}1\\1\\1\end{bmatrix} \quad (17)$$

$\{\boldsymbol{f}\}$ is the global boundary flux vector which is assembled from the elemental boundary flux vectors $\left\{f_L^e\right\}$ that can be given as

$$\left\{f_L^e\right\}=\int_{\Gamma}\frac{1}{T}\left(T^e\frac{\partial \hat{h}_L^e}{\partial x}n_x+T^e\frac{\partial \hat{h}_L^e}{\partial y}n_y\right)N_L^e\,d\sigma^e=\left(\frac{bq_x^e}{T^e}\left(\frac{d\sigma_y^e}{2}\right)+\frac{bq_y^e}{T^e}\left(\frac{d\sigma_x^e}{2}\right)\right)\begin{bmatrix}1\\1\\1\end{bmatrix} \quad (18)$$

From the known head distribution at previous time level the unknown head distribution at the next time level is obtained by recursively solving the set of algebraic equations given in Equation (11).

V. RESULTS AND DISCUSSION

The chosen Test Case is aimed at validating the FEFLOW model. The validation of flow models is accomplished by comparing model simulations with the reported analytical solutions **[*Illangasekara and Doll, 1989*]**. This test case enables the investigations of the response of the aquifer to varying discharge rates from the pair of pumping wells. Further the sensitivity of FDFLOW and FEFLOW solutions to the variation in aquifer parameters such as transmissivty, specific yield and time step size is analyzed. For Test Case a rectangular, homogeneous, and isotropic unconfined aquifer is chosen as shown in Figure 1.The rectangular aquifer is selected mainly to satisfy the shape constraints imposed for the analytical solution. The aquifer system is

3,200 m long and 2,800 m wide. The head at the top and bottom sides of the aquifer boundary is considered to have constant value of 100 m throughout the simulation, and left and right sides of the aquifer boundary is considered to have zero groundwater flux. Two pumping wells are placed at a location of (1400 m, 1400 m) and (1800 m, 1400 m) from the origin, as shown in Figure 1. Initially the groundwater head is assumed static with a value of 100 m at all nodes in the aquifer domain. The water table drawdown caused by pumping are observed at an observation well situated at a location of (1000 m, 1000 m) from the origin. The aquifer parameters used in the simulation include aquifer thickness (b =30 m), constant pumping rates for the two pumping wells (Q_{p1} & Q_{p2} = 1142.85 & 1428.57 m3/d), effective porosity (θ =0.30), aquifer transmissivty (T =885.71 m2/d) and specific yield (S_y =0.15), respectively. For FDFLOW model, the aquifer is discretized using mesh centered finite difference grid which results into 255 computational cells with uniform nodal spacing of 200 m in both x- and y- directions as shown in Figure 1. For FEFLOW model, the aquifer is discretized using the triangular finite element mesh with 448 elements. The size of the square finite difference cell and isosceles triangular element is 200 m. Total nodes with Dirichlet boundary condition and Neumann boundary conditions are 32 and 28, respectively.

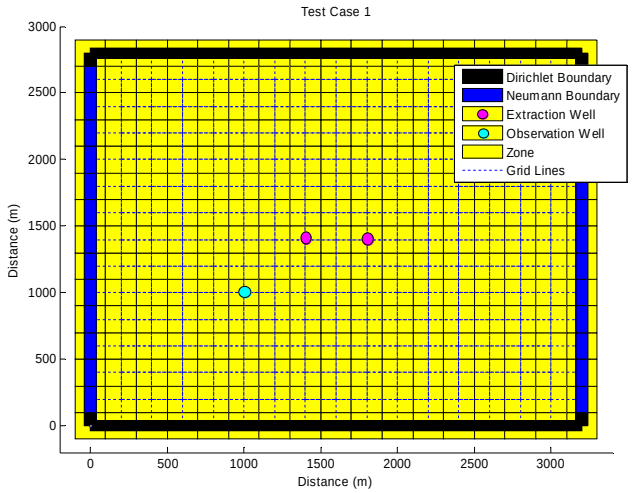

Figure 1 *Schematic of aquifer modeled in Test Case for the simulation of two-dimensional transient groundwater flow in un confined aquifer under the pumping well conditions*

Validation of FDFLOW and FEFLOW models:

The water table drawdown values at an observation well due to the pumping by pair of wells for 210 days are computed by FDFLOW and FEFLOW models. The time- drawdown curves obtained by FDFLOW and FEFLOW models and reported analytical solution [*Illangasekare and Doll, 1989*] are compared as shown in Figure 2.

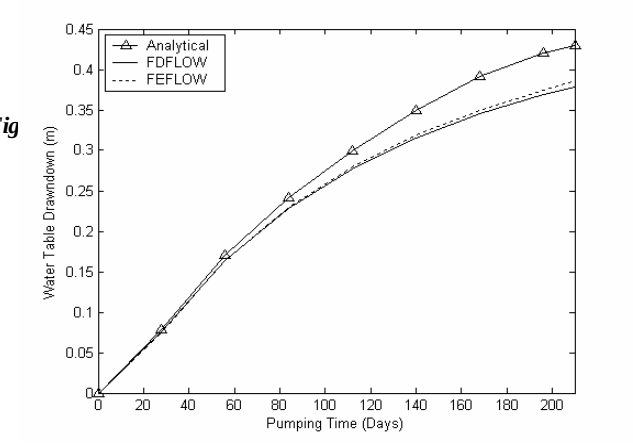

Fig ***se***

The drawdown values are computed as 0.38 and 0.39 m by FDFLOW and FEFLOW models, respectively which are in close agreement with the reported drawdown of 0.42 m by analytical solution [*Illangasekare and Doll, 1989*] implying the validity of the developed flow simulation models. The time step size is taken as 7 days to meet the Courant number criterion for FDFLOW model. It is also seen from the comparison of drawdown curves that in the initial stages of the simulation both the numerical and analytical solutions are almost same but in later stages of the simulation the FDFLOW solutions deviate appreciably from

analytical solution. The percentages of the difference between FDFLOW and FEFLOW and analytical solutions are 9.5 % and 7.2% respectively. This difference is acceptable in groundwater flow modeling. using a mesh-centered finite difference grid. The nodal spacing in x- and y- direction is kept uniform as 5 m. The total nodes in the finite difference grid are 255 while the total boundary nodes are 60.

Comparison of head distribution by FDFLOW and FEFLOW models:

The head distribution obtained by FDFLOW model compares favorably with the head distribution obtained by FEFLOW model. It is observed from Figure 3 that the contours of 99.4, 99.5 and 99.6 m head obtained by both the models are not affected by boundary effects however the contour of 99.7 m head has shown some numerical dispersion due to the presence of impervious boundary on the left and right sides of the aquifer. The FEFLOW simulations caused greater deviation of 99.7 m head contour because of the numerical error in the approximation of the boundary flux terms by linear interpolation functions.

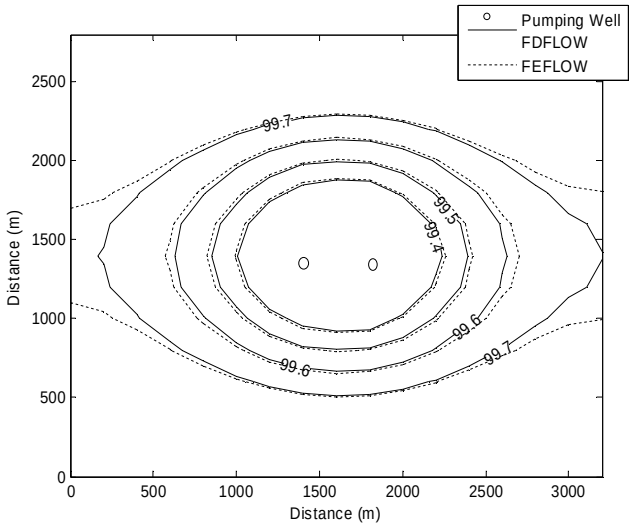

Figure 3 *Comparison of groundwater head distributions by FDFLOW and FEFLOW models under the pumping well conditions for Test Case*

Effect of transmissivity on water table drawdown:

Figure 4 shows the effect of the varying magnitude of the transmissivity on the water table drawdown computed by FDFLOW and FEFLOW models. The drawdown values computed by FDFLOW model are 0.47, 0.93 and 0.37 m for the transmissivities of 885.71, 442.85 and 1107.14 m^2/d respectively.

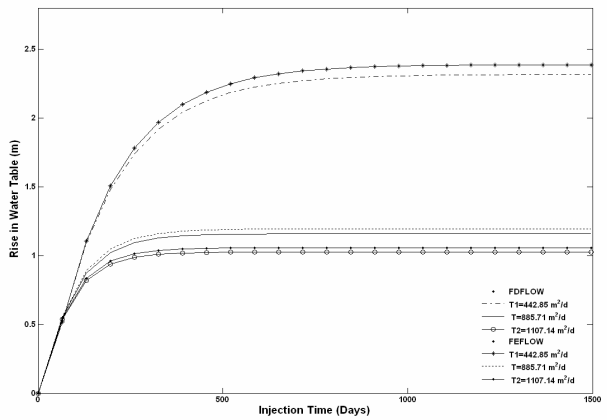

Figure 4 *Effect of transmissivity on water table drawdown for Test Case*

The corresponding values of the water table drawdown obtained by FEFLOW model are 0.48, 0.96, and 0.38 m, respectively. Thus it is inferred from the results that the 50% decrease in the magnitude of the transmissivity causes drawdown to be doubled and 25 % increase in the magnitude of the transmissivty causes the drawdown to get lowered by 25 %. These results are on the expected lines as in well-drawdown equation, transmissivity in denominator plays more important role than a function of loga-

rithmic transmissivty in Jacob's equation $s = \frac{Q_p}{4\pi T} \ln \frac{2.25 T t}{r^2 s}$ or a well function transmissivity in Theis equation $s = \frac{Q_p}{4\pi T} w(u)$

where the parameter in well function is $u = \frac{r^2 S}{4Tt}$, where $W(u)$ the well function is and r is the radius of influence.

Effect of specific yield on water table drawdown:

Figure 5 shows the comparison of water table drawdown curves obtained by FDFLOW and FEFLOW models with the effect of variation in specific yield magnitude. The specific yield is varied from the base value of 0.15 to 40% less of that value i.e. 0.09 and 100% more of that value i.e. 0.30.

Corresponding to these values the drawdown computed by FDFLOW are 0.47, 0.471, and 0.469 m where as for the same range of the specific yield variation the drawdown computed by FEFLOW are 0.483, 0.484, and 0.481m. It has therefore been inferred from the results that the change in specific yield has insignificant effect on the drawdown. But as it is evident from the result analysis that increase in specific yield results in reduction in the drawdown as compared to increase in drawdown caused by decrease in the specific yield. This is due to the fact that unlike transmissivity, specific yield term is only a parameter of the well function and does not show direct proportionality with drawdown in a well response equation.

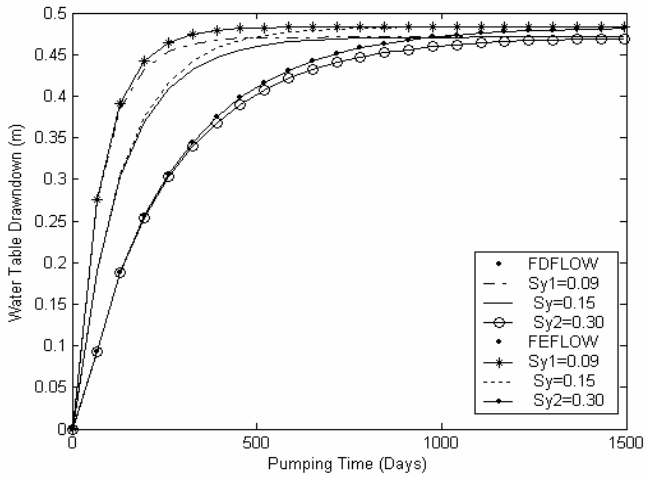

Figure 5 *Effect of specific yield on water table drawdown for Test Case*

Effect of pumping rate on water table drawdown:

The influence of the change in the well pumping rates over water table drawdown is shown in Figure 6.

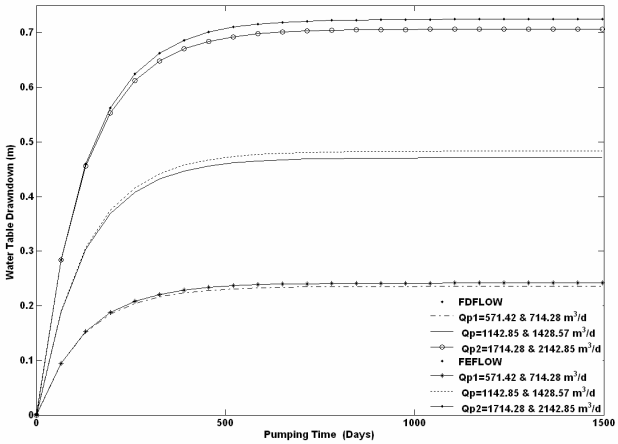

Figure 6 *Effect of pumping rate on water table drawdown for Test Case*

The range of variation in pumping rates of well 1 and 2 is considered as + 50% and -50% of the initially chosen pumping rates. It can be seen from the Figure 6 that for 50% decrease in the given pumping rate has causes the decrease in drawdown by 51 % and 50% by FDFLOW and FEFLOW models, respectively whereas 50% increase in the given pumping rate causes the increase in drawdown by 48.93 % and 49.89% by FDFLOW and FEFLOW models, respectively. It is further noticed that the rate of

change in drawdown is maximum till the 500 days after the start of pumping there after the drawdown are found to be stabilized thus groundwater flow regime is approaching the steady state. These results are on expected lines from practical considerations.

Effect of Courant number on water table draw down :

The influence of the change in the well pumping rates over water table drawdown is shown in Figure 7. The time step sizes are taken as 0.5 and 1 day, respectively. The corresponding Courant numbers are calculated as 0.09 and 0.15, respectively which are well below the permissible value of unity. FDFLOW model computes the drawdown of 0.388 and 0.378 m for the time step sizes of 0.5 and 1 day, respectively after 150 days of pumping whereas FEFLOW model computes the drawdown of 0.392 and 0.385 m for the for the corresponding values of time step size. Thus it is inferred from the results that even 50% increase in time step size has negligible effect on the drawdown. The size of time step greater than 1.1 days results in unstable solutions due to violation of stability criteria. Hence, for given transmissivty, specific yield and aquifer discretization the time step size of 1 day is recommended.

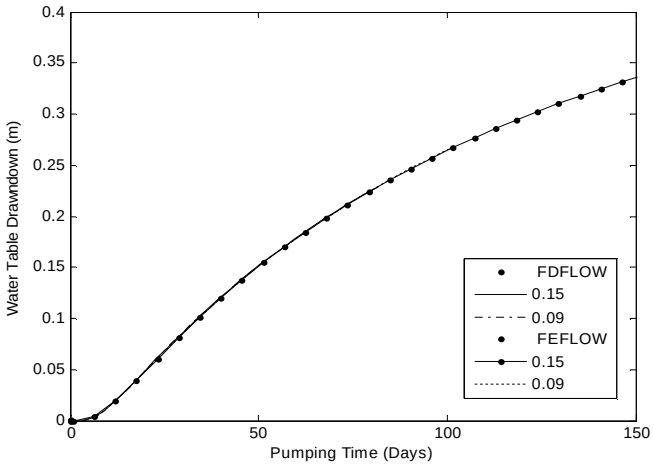

Figure 7 *Effect of Courant Number on water table drawdown for Test Case*

VI. CONCLUSIONS

The following are the conclusions of the present study:
Validation of FDFLOW and FEFLOW model for chosen Test Case shows that there is a close agreement between computed and analytical solutions in the initial stages of the pumping, however, after 210 days of pumping the difference between drawdown obtained by FDFLOW and FEFLOW model and analytical solution are 10% and 7% respectively. Thus FEFLOW model has performed better than FDFLOW model. The deviation of FEFLOW computed solutions from analytical solutions in the later stages of simulation may be attributed to lower order interpolation function used in the FEFLOW model. For chosen Test Case , the FDFLOW and FEFLOW model solutions are found to be stable for the Courant number of 0.14 for the chosen time step of 1 day.FDFLOW and FEFLOW solutions are more sensitive to pumping rate and moderately sensitive to the transmissivity of the aquifer, whereas the effect of the specific yield is found to be negligible over the numerical solutions.

VII. REFERENCES

[1] Pinder, G. F., and Bredehoeft, J. D., 1968, Application of the digital computer for evaluation of aquifer, *Water Resources Research*, 1069-1093.
[2] Pinder, G. F., and Frind, E. O., 1972, Application of Galerkin's procedure to aquifer analysis. *Water Resources Research*, 8(1):108-120.
[3] Narasimhan, T. N., and Witherspopoon, P. A., 1976, An integrated finite difference method for analyzing fluid flow in porous media, *Water Resources Research*, 12(1): 57-64.
[4] Wang, H. F., and Anderson, M. P., 1982, *Introduction to Groundwater Modeling*, W. H. Freeman and Company, New York.
[5] Thomson, B. M., 1984. Techniques for making finite elements competitive in modeling flow in saturated porous media. Water Resources Research: 1099-1115.
[6] Illangasekare, T. H., and Doll, P., 1989, A discrete kernel method of characteristics model of solute transport in water table aquifers, *Water Resources Research*, 25(5): 857-867.
[7] Serigo, F., et al., 2004, Application of the discontinuous spectral Galerkin method to groundwater flow, *Advances in Water Resources*, 27: 129- 140.
[8] Kulkarni, N.H. and Rastogi, A.K., 2012, Numerical Experiments on Solute Transport in Groundwater Flow System, *International Journal of Emerging Technology and Advanced Engineering*, 2(8): 108-413.